PHYSICAL REVIEW E **70**, 026307 (2004)

Reaction front propagation in a turbulent flow

Christophe R. Koudella*

Department of Applied Mathematics and Theoretical Physics, Centre for Mathematical Sciences, University of Cambridge, Cambridge, CB3 0WA, United Kingdom

Zoltán Neufeld†

Center for Nonlinear Studies, Los Alamos National Laboratory, Los Alamos, New Mexico 87545, USA

(Received 21 July 2003; revised manuscript received 6 January 2004; published 26 August 2004)

The propagation of reaction fronts in a turbulent fluid flow is studied by direct numerical simulations in two space dimensions. The velocity field is obtained from integrating the Navier-Stokes equation in two dimensions. We investigate the structure of the reaction front and the enhancement of the front propagation speed due to turbulent mixing. Consistently with earlier theoretical, predictions and experiments we find two qualitatively different regimes as the Damköhler number—the ratio of eddy turnover times and of the characteristic chemical time scale—is varied, corresponding to a distributed reaction zone and thin wrinkled fronts.

DOI: 10.1103/PhysRevE.70.026307 PACS number(s): 47.70.Fw

I. INTRODUCTION

The mixing of passively advected scalar fields in turbulent fluid flows has wide ranging applications of fundamental and practical importance and significant theoretical progress has been made throughout the last decade [1–3]. In many applications species passively advected by a fluid flow participate at the same time in chemical reactions or biological processes. While the effect of mixing on chemical or biological activity in simple—laminar or chaotic—flows has received considerable attention recently [4], comparatively little work has been done on reactive passively advected species in multiscale turbulent flows.

One of the simplest classes of chemical reaction dynamics taking place in a fluid environment is the first-order autocatalytic process of the type $A+B\rightarrow 2B$, where reactant B consumes component A. It is well known that in extended reaction-diffusion systems this kind of process leads to the formation of propagating reaction fronts [5]. Analogous fronts also exist in models of combustion (flames) [6,7] or biological populations [8] (e.g., oceanic plankton ecosystems).

Front solutions are typical to models where the reaction dynamics has multiple steady or quasisteady states [9]. The dynamics of the front can be described by nonlinear diffusion equations of the form

$$\frac{\partial \theta}{\partial t} = D\nabla^2\theta + \alpha\, f(\theta), \tag{1}$$

where $\theta(\mathbf{r},t)$ is a scalar concentration field, also termed progress variable, taking on values $0<\theta(\mathbf{r},t)<1$, and $f(\theta)$ is a reaction term that satisfies

$$f(\theta=0)=f(\theta=1)=0, \tag{2}$$

where $\theta=0$ and $\theta=1$ represent two different phases of the system.

A classic model of front propagation and perhaps the simplest one is the so-called Fisher-Kolmogorov-Petrovsky-Piskunov (FKPP) equation, initially introduced as a model for the propagation of an advantageous gene in a population [10,11]. The FKPP model effectively describes the invasion of an unstable phase ($\theta=0$) by a stable one ($\theta=1$) using a quadratic reaction term $f(\theta)=\theta(1-\theta)$. For the first-order autocatalytic reaction, the scalar field θ can be interpreted as the local relative concentration of reactant B, $C_B/(C_A+C_B)$. There exist similar front solutions for models of higher order autocatalytic reactions like $A+nB\rightarrow(n+1)B$ with corresponding reaction term $f(\theta)=\theta^n(1-\theta)$. In the case of combustion θ is a normalized temperature field and the two phases represent the fresh mixture of fuel and oxidizer at low temperature and the completely burnt state at high temperature, respectively. The reaction rate depends on the temperature according to the Arrhenius law, resulting in an exponential form of the source term.

Equation (1) has planar traveling front solutions propagating at constant speed $v_f=|\mathbf{v}_f|$ with no change of shape so that $\theta(\mathbf{r},t)=\theta_f(\mathbf{r}-\mathbf{v}_f t)$. Dimensional analysis shows that the minimum or critical speed is $v_0=C_0(\alpha D)^{1/2}$. The value of the constant C_0 depends on the form of reaction term and can be obtained analytically for quadratic and cubic autocatalysis as $C_0^{(n=1)}=2$ and $C_0^{(n=2)}=1/\sqrt{2}$. Note that planar fronts may also exist for speeds larger than v_0 [12,13]. In the case of an initial value problem it may be shown that planar fronts propagate at the critical speed v_0 provided the initial condition on θ is localized or decays in space sufficiently fast. At critical front speed conditions the front propagation mechanism is initiated by diffusive transport at the leading edge of the front. However, for supercritical front speed conditions the mechanism is not diffusion initiated, but differs in that a local transition from $\theta=0$ to $\theta=1$ occurs at different points ahead of the front with a time delay, the reaction front speed

*Present address: Division of Engineering and Applied Sciences, Harvard University, Cambridge, MA 02138, USA. Electronic address: ckoudell@deas.harvard.edu

†Electronic address: zoltan@cnls.lanl.gov

determining delay itself being controlled by the precise shape of the initial condition. Consequently any meaningful numerical experiments ought to take into account the "sensitivity to initial conditions:" of the front propagation speed, without which uncontrolled transients may bias the experimental results and furthermore it is preferable to select initial conditions guaranteeing the critical speed as the steady state front speed.

In the presence of a fluid flow the evolution of a passively advected, reactive scalar field is governed by an advection-reaction-diffusion equation written in nondimensional variables as

$$\frac{\partial \theta}{\partial t} + \mathbf{v} \cdot \nabla \theta = \mathrm{Pe}^{-1} \nabla^2 \theta + \mathrm{Da}\, f(\theta), \tag{3}$$

where $\mathbf{v}$ is a prescribed velocity field dependent on space and time only. Further, for characteristic length and velocity scales, L and U, $\mathrm{Pe}=U/LD$ and $\mathrm{Da}=L\alpha/U$ are the dimensionless Péclet and Damköhler numbers, respectively. The Péclet number represents the ratio of advective and diffusive transport, while the Damköhler number is the ratio of the characteristic time scales of advection and reaction. Also note that the dimensionless time is scaled by the characteristic advective time scale $T=L/U$. For concreteness we may assume that L is the integral scale of the flow and U is the root-mean-square velocity obtained from a spatial average.

The autocatalytic process described by Eq. (3) has been investigated for the case of unsteady laminar flows in bounded domains [14] and open flows with a bounded mixing region [15]. Front propagation in simple steady laminar flows was studied recently in Refs. [16–18]. For the case of steady cellular flows it was shown that for small diffusivity ($\mathrm{Pe} \gg 1$) in the slow reaction regime ($\mathrm{Da} \ll 1$) the front speed scales as $v_f/v_0 \sim \mathrm{Pe}^{-1/4}$, independent of Da, while for fast reactions ($\mathrm{Da} \gg 1$), the front speed scales as $v_f/v_0 \sim \mathrm{Pe}^{-1/4}\mathrm{Da}^{-1/2}$ [16]. In another recent work [19] rigorous bounds for FKPP front propagation speeds in simple flow geometries have been derived. More closely related to the present study are the investigations of front propagation in a two-dimensional stochastic field generated by integration of a stochastic differential equation [20,21] and meant to represent a synthetic turbulent velocity field. This work uses a source representing a cubic autocatalytic reaction $k\theta^2(1-\theta)$ and focuses primarily on qualitative properties of reaction fronts generated by synthetic velocity fields. Two types of generic geometries for the reaction zones are described there, namely the distributed reaction zone and the sharp wrinkled front for increasing flow intensities while the reaction rate is kept constant. The existence of these two regimes was first predicted by Damköhler [22] and was later observed in laboratory experiments [23].

The so called G-equation limit of Eq. (3) corresponding to a geometrical optics approximation obtained in the limit $\mathrm{Da} \to \infty$, $\mathrm{Pe} \to \infty$, and $\mathrm{Da}/\mathrm{Pe} = \mathrm{const}$ describes the propagation of thin reaction fronts [7,24]. The advantage of the G equation is that it is amenable to analytical (asymptotic) treatment for steady or unsteady cellular flows as shown in Ref. [25] and to scaling analysis for turbulent flow [26].

In the present work we study the effects of incompressible steady-state Navier-Stokes turbulent velocity fields on the propagation dynamics of fronts governed by Eq. (3) by direct numerical simulations. The numerical tool we developed allows us to systematically study the speed-up of reaction fronts by turbulent fluid mixing in transient and stationary reaction regimes for a specific range of reaction rates. With respect to the turbulent velocity field time scales we simulate, we focus in particular on the transition from slow reaction rates with broad fronts to moderately fast reaction rates with sharp fronts, but we do not approach the G-equation limit in the sense that no reaction considered is much faster than the fastest turbulent time scale in the flow. In Sec. II we describe the numerical model and the experimental setup we used. Section III presents our results and a discussion of our findings. We conclude the report in Sec. IV.

II. NUMERICAL METHODS AND EXPERIMENTAL SETUP

A. Turbulence model

While it is often stressed that real fluid flows from turbulent scales down to molecular diffusive scales are intrinsically three dimensional, we presently wish to explore generic effects of multiscale turbulent flow fields on front propagation. Therefore, we simplify the problem by working in the plane and we consider the front dynamics in a two-dimensional incompressible turbulent velocity field. Two-dimensional turbulent flows are also relevant in geophysical context. We consider a fluid flowing in the (x,y) plane governed by the two-dimensional Navier-Stokes equation in the vorticity formulation

$$\frac{\partial \zeta}{\partial t} + \mathbf{v} \cdot \nabla \zeta = \tau_{\mathrm{drag}} + \mathrm{Re}^{-1} \nabla^{\mathbf{n}} \zeta + \tau, \tag{4}$$

where ζ is the scalar vorticity, $\zeta = (\nabla \times \mathbf{v}) \cdot \mathbf{k}$, $\nabla = (\mathbf{i}\partial/\partial \mathbf{x}, \mathbf{j}\partial/\partial \mathbf{y})$ and $\mathbf{k}$ is a unit vector defining the z direction perpendicular to the flow plane. Further, τ_{drag} is a drag moment acting as a vorticity sink, $\mathrm{Re}=U/L\nu_{\mathrm{hyper}}$ is the Reynolds number based on the hyperdiffusion coefficient ν_{hyper} and appears as a coefficient multiplying the nth-order hyperdissipation operator ∇^n and τ is a force curl acting as a vorticity source. The significance of these right-hand-side terms is explained in what follows. The vorticity field is related to the velocity field via the scalar streamfunction $\psi(x,y,t)$ following the relations $\zeta = -\nabla^2 \psi$, $u = \partial\psi/\partial y$ and $v = -\partial\psi/\partial x$.

Equation (4) was integrated on a doubly periodic domain of size $2\pi \times 2\pi$ with a spatial resolution of 1024^2 gridpoints using a classic Fourier-Galerkin spectral method, but with a recently proposed formulation for the vorticity sink τ_{drag}. We assume that the most crucial statistical properties of three-dimensional multiscale turbulent flows are best mimicked within a two-dimensional approximation when we consider a velocity field with spectral properties corresponding to the so called inverse (upscale) energy cascade range of two-dimensional turbulence [27,28]. The energy spectrum in this regime is known to be described by the same power law as the inertial range spectrum of three-dimensional Kolmog-

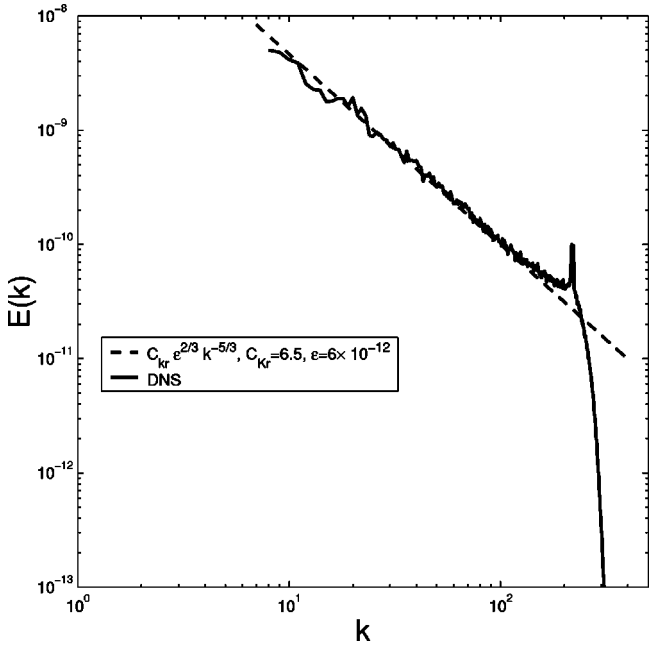

FIG. 1. Instantaneous kinetic energy spectrum of the turbulent velocity field.

orov 1941 turbulence and scales as $k^{-5/3}$. A method for generating just such a flow is described in Ref. [29], SGC for short, and we follow this approach closely in the present work. SGC showed that it is possible to generate an inverse energy cascade in a bounded two-dimensional flow displaying the same scaling behavior as that conjectured by Kraichnan for an unbounded flow by introducing one forcing mechanism and two dissipation channels. The force curl, τ in Eq. (4), is acting at small scales in a narrow wave number band and is δ correlated in time. The first dissipation channel τ_{drag} is a large-scale closure scheme based on the EDQNM approximation and acts as a large-scale energy sink compatible with the required $k^{-5/3}$ scaling up to the largest resolved scales. In this respect the approach of SGC differs from all other upscale energy cascade numerical studies of two-dimensional turbulence known to us, which consistently use *ad hoc* large scale friction schemes. The second dissipation channel is a strong high-order harmonic hyperdissipation function strongly suppressing vorticity fluctuations associated with the direct (downscale) flux of vorticity. Full details of the numerical model may be found in Ref. [29]. Note that we use numerical parameters identical to those used in the original publication validating the numerical scheme. Remarkably, due to the interplay between the two dissipation channels the resulting flow field is maintained void of coherent structures for arbitrary times and a forced-dissipative equilibrium simulation is obtained. We illustrate the resulting stationary energy spectrum in Fig. 1 where it is seen that we obtain the Kraichnan 1967 scaling between wave numbers $k=8$ and $k=215$ as $E(k)=C_{\mathrm{Kr}}\epsilon^{2/3}k^{-5/3}$ with $C_{\mathrm{Kr}}\approx 6.5$. It is in this stationary flow that we consider the advection-reaction-diffusion problem whose numerical model is discussed next.

B. Passively advected reactive species model and experimental setup

While the Fourier-Galerkin spectral method used for the turbulent flow simulation has desirable convergence properties, it is unfortunately not suitable for the integration of the reactive species. Indeed, in virtue of an unstable (or marginally stable) fixed point $\theta=0$ in the reaction dynamics, it is desirable to adhere to a positive definite numerical method. We found that the use of a sixth order compact finite difference method for the spatial derivatives [30] leads to satisfying results. While the resulting spatial scheme is not strictly positive definite, compact finite difference schemes nevertheless have a good track record for the solution of species equations in various direct-numerical-simulation/large-eddy-simulation studies of turbulent combustion problems [31]. We couple the reactive part to the advection-diffusion part of Eq. (3) via a straightforward Strang splitting scheme and perform the time integration with a second or fourth order Runge-Kutta scheme.

Generating time series of stationary progressive reaction fronts requires the development of a stable numerical model in order to be able to integrate the system (4) and (3) over arbitrary long times. This is due to the existence of a transient regime when starting a front propagation experiment from a given initial condition on one hand, and the presence of rather important fluctuations of the turbulent front propagation speed v_T around its mean value on the other hand, as shall be detailed in Sec. III. Given the relatively small size of the computational domain as defined in the laboratory frame, the finite front propagation speed and the long integration times required to overcome the earlier-mentioned constraints, we developed a framework operating in a moving reference frame, to be described in what follows. Let us consider the solution of Eq. (3) in a domain periodic in the y direction and unbounded in the x direction. The boundary conditions on the scalar are taken to be $\theta(x\to-\infty,y,t)=1$, $\theta(x\to\infty,y,t)=0$, corresponding to the presence of a sink at $x\to-\infty$ and of a source at $x\to\infty$. The turbulent flow is mapped onto this domain by periodic repetition of the velocity field along the x axis, so that $\mathbf{v}(x+2\pi,y)=\mathbf{v}(x,y)$. We consider three different types of reaction terms corresponding to quadratic and cubic autocatalysis and an exponential form that is analogous to flame fronts in premixed combustion

$$f(\theta)=[\theta(1-\theta),\theta^2(1-\theta),(1-\theta)\exp(-1/\theta)]. \tag{5}$$

We now define the instantenous front speed based on the bulk reaction rate as in Ref. [19]:

$$v_T=\frac{1}{L_y}\int_{-\infty}^{+\infty}\int_0^{L_y}\frac{\partial\theta}{\partial t}dxdy. \tag{6}$$

By substituting Eq. (3) into Eq. (6) and observing that the integrals of the advective and diffusive transport terms vanish along both directions (assuming zero mean flow in the x direction and periodic boundary conditions in the y direction) we obtain

$$v_T = \frac{\mathrm{Da}}{L_y}\int_{-\infty}^{+\infty}\int_0^{L_y} f(\theta)dxdy, \tag{7}$$

which identifies a relationship between the scalar field θ and the instantenous front propagation speed. Since the earlier integral has contributions coming from the frontal region only, the front speed can be approximated by restricting the outer integral to a finite interval L_x centered around the front, provided L_x is sufficiently large, so that outside this interval θ is very close to the unreacted $\theta=0$ or completely consumed $\theta=1$ states. In the regions far behind and far ahead of the propagating front where the scalar field is almost uniform in space ($\theta=1$ and $\theta=0$, respectively), mixing has no effect and there can be no contribution from these regions to the dynamics of the reactive species. The region where the reaction is active, however, is changing in time advancing along the x axis. In order to maintain the front in the center of the computational domain, we therefore consider the Galilean transformed rectangular domain (x',y) of size $L_x=n2\pi, L_y=2\pi$, moving with the instantaneous front speed, v_T so that

$$x' = x - \int_0^t v_T(\tau)d\tau. \tag{8}$$

The boundary conditions are periodic in y and the x'-boundary conditions are $\theta(x'=0,y)=1, \theta(x'=L_x,y)=0$. The length of the domain, L_x, is chosen to be much larger than the width of the front so that the presence of the boundaries have negligible effect on the propagation speed. In practice doubling the basic $2\pi\times 2\pi$ square ($n=2$) is sufficient for most front widths considered in the present study. The speed of the moving reference frame, is set by the constraint that the first moment of the progress variable within the computational domain keeps a constant value

$$\langle\theta\rangle(t) \equiv \frac{1}{L_xL_y}\int_0^{L_x}\int_0^{2\pi}\theta(x',y,t)dx'dy = \frac{1}{2}. \tag{9}$$

This condition ensures that the front stays in the center of the computational domain and it allows us to make integrations over arbitrarily long times as required in order to obtain good samples of arbitrary quality of the fluctuating front speed.

Preliminary numerical experiments with various initial conditions have shown that the initial adjustment phase toward a stationary propagating front is strongly dependent on initial conditions. The dependence is related to the width of the initial condition compared to the width of the stationary front. In order to avoid these artificial transient effects we selected the stationary front solutions of the reaction-diffusion Eq. (1) as initial conditions in Eq. (3). The initial conditions were obtained from numerical integration of the corresponding one-dimensional reaction-diffusion equation in a stationary medium ($\mathbf{v}=0$) using a step function as initial condition.

For a given statistically steady turbulent velocity field and a given value of Pe we focus on the Da dependence of the fronts. The maximum admissible value for Pe (i.e., the smallest species diffusivity avoiding spectral blocking on the discrete mesh) was determined by considering a series of runs of a forced passively advected and chemically inert species. There the Pe number was increased so as to obtain a qualitatively sound Obukhov $k^{-5/3}$ scaling range and a diffusion range for the species variance spectrum. The resulting numerical value selected was $\mathrm{Pe}=1.6\times 10^3$. It was then found experimentally that in the case of the reactive species the Pe had to be lowered somewhat to a value of $\mathrm{Pe}=1.244\times 10^3$. Indeed the source term is a variance production term and an increased species diffusivity is necessary to avoid spectral blocking at the smallest scales. We estimated the Damköhler numbers Da to be considered with respect to turbulent time scales estimated from the kinetic energy spectrum. To first approximation we can associate a characteristic time scale $\tau(k)$ to each length scale $L\sim 1/k$ in the flow using the kinetic energy spectrum. From dimensional analysis we find that that $\tau(k)\sim 2C_{\mathrm{Kr}}^{-1/2}\epsilon^{-1/3}k^{-2/3}$. For the inverse cascade simulated presently with k in Ref. [8] (p. 215) we get time scales in the range $\tau_{\min}\approx 0.033, \tau_{\max}\approx 0.30$. The Damköhler number has been varied in the range $0.025<\mathrm{Da}<12.8$, that represents reaction timescales, $\tau_r\sim \mathrm{Da}^{-1}$ slower or comparable to the turbulent time scales. For small Da the reaction is very slow, therefore a very long time is needed to reach the stationary regime of the front propagation, but their treatment is unproblematic. However, the range of attainable Da is bounded earlier by the fact that fronts becomes very sharp at high values. Computing extreme cases and thereby resolving the sharp fronts requires either higher spatial resolutions of the numerical model or the use of altogether alternative numerical schemes allowing the representation of quasidiscontinuities. Also note that in the case of the quadratic reaction term $\theta(1-\theta)$, due to the instability of the unreacted phase (unstable fixed point at $\theta=0$), the highest Da that could be achieved with the present numerical method based on sixth order compact finite difference schemes was 1.6.

III. RESULTS AND DISCUSSION

The turbulent flow distorts the initial planar front and produces a complex front structure. It thus increases the area over which the reaction is active, enhancing the bulk reaction rate and the front propagation speed.

After a transient acceleration time the turbulent front speed saturates and reaches a statistically stationary state. The instantenous front speed, based on the bulk reaction rate was obtained from the scalar field $\theta(\mathbf{r},t)$ according to Eq. (7). The temporal evolution of the front speed in the turbulent flow is shown in Fig. 2 for some representative values of the Damköhler number Da for quadratic autocatalysis.

All qualitative features of the front dynamics and the structure of the fronts in the stationary state were found to be very similar for the three types of reaction dynamics considered. There are, however, differences in the numerical values of the propagation speed.

The average front speed in the stationary regime increases with Da and the time needed to reach the statistically stationary state is longer for small Da. Even in the stationary state the instantaneous front speed fluctuates in time. These fluctuations are stronger when the reaction is fast (see Fig. 2). We believe that the fluctuations of the propagation speed are

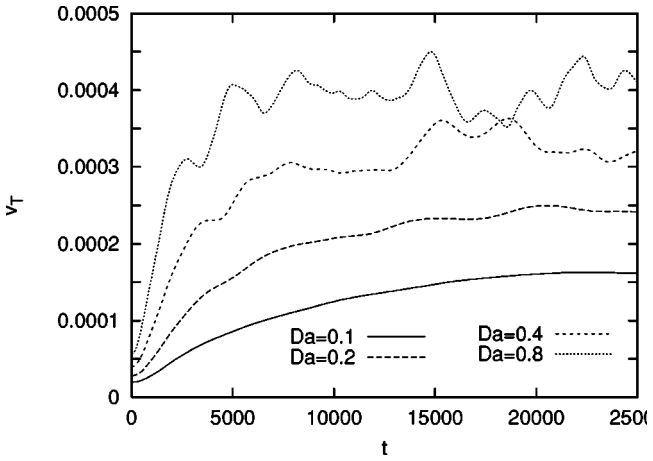

FIG. 2. Instantenous front speed as a function of time obtained from the bulk reaction rate $[f(\theta)=\theta(1-\theta)]$.

related to the finite width of the channel. The size of the largest coherent structures within the front is set by the integral scale, $L=\pi/4$, of the turbulent flow (the characteristic size of the largest eddies). In our simulations the width of the channel is only eight times larger than the integral scale. In a much wider channel, $L_y \gg L$, the fluctuations would presumably average out and lead to an almost constant propagation speed. However, numerical simulations in a much wider channel and the generation of turbulent flow over scales much larger than the integral scale would be computationally very expensive and require additional memory afforded only by the use of distributed computing. Therefore, we use an alternative approach by performing simulations over a long time period, so that a well defined average front speed can be determined. It is assumed, that this time-averaged front speed is not sensitive to the width of the channel and is the same as the constant asymptotic front speed corresponding to the limit $L_y \to \infty$.

Snapshots of typical front structures in the stationary regime are presented in Fig. 3 for three different reaction rates. When Da is small the reaction zone is broad, extending over distances larger than the integral scale along the x direction. This explains the long transient time necessary to buildup the broad front structure. In case of larger Damköhler numbers the front structure becomes sharper and the reaction zone is confined to a narrow region. The average front profiles, obtained by averaging the concentration field along the y axis (Fig. 4) shows the broadening of the front along the x direction as Da is decreased.

Apart from a change in the width of the reaction zone, the fluctuations in the transverse direction also depend on the Damköhler number. This can be characterized by the probability density function of the scalar $p_{\theta_0}[\theta(x=x_0,y)]$ along transects $x=x_0$ corresponding to different average values of the progress variable, $\langle\theta(x=x_0,y)\rangle=\theta_0$ (Fig. 5). For slow reactions the pdfs are distributed in a small interval around the mean θ_0. When the Damköhler number is large the distributions are mainly concentrated to the extreme values, $\theta=0$ and $\theta=1$, and the probability of intermediate concentration values is rather small.

The main quantity of interest is the time-averaged front speed and its dependence on the reaction rate. The front

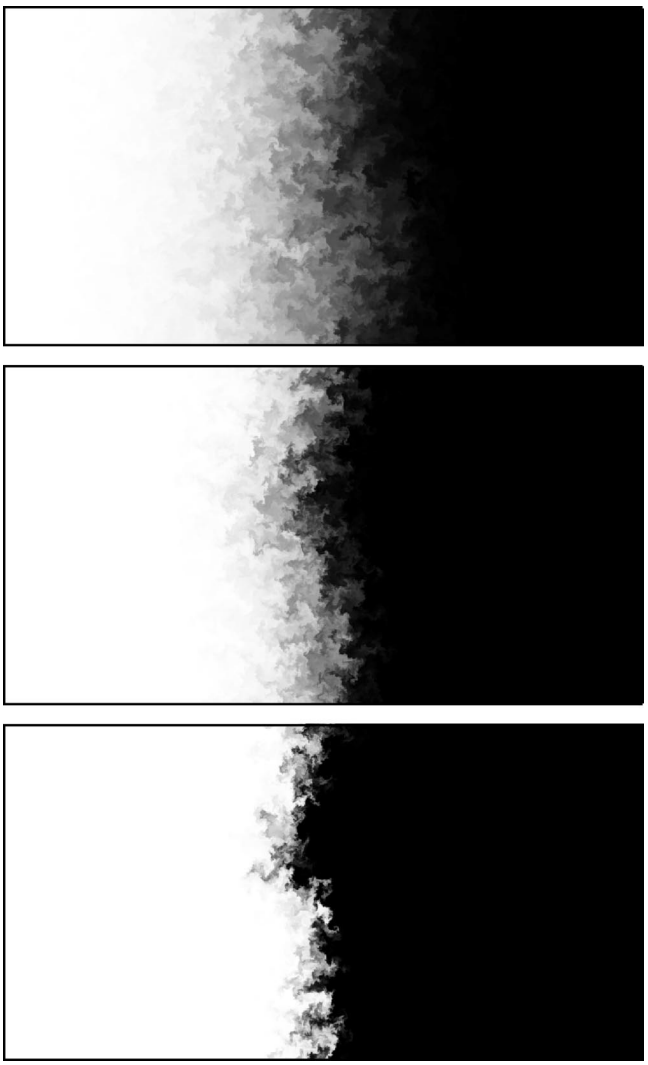

FIG. 3. Snapshots of the front structure $\theta(x,y)$ for $f(\theta)=\theta(1-\theta)$, after a statistically stationary state has been reached. The values of the Damköhler numbers are 0.05, 0.2 and 0.8 (from top to bottom).

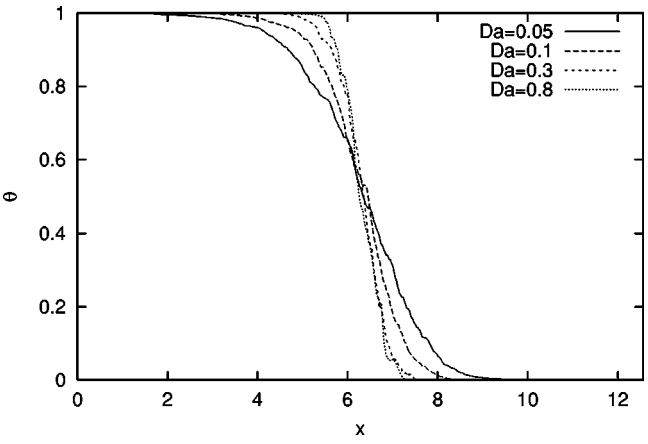

FIG. 4. Front profiles obtained by calculating the average concentration along the direction transverse to the propagation (y axis).

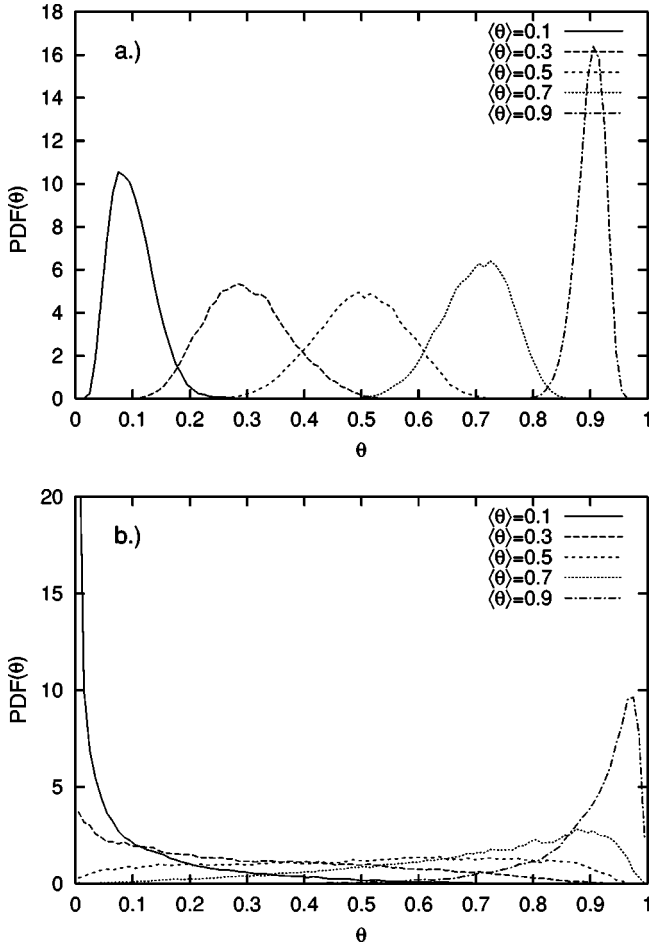

FIG. 5. Probability density functions of the concentration θ along transects taken in the direction perpendicular to the propagation: (a) slow reaction Da=0.05 and (b) fast reaction Da=0.4.

speed normalized by the rms velocity in the turbulent flow is presented in Fig. 6 for the three different types of source terms stated in Eq. (5) earlier. The vertical bars show the standard deviation of the fluctuating front speed in the stationary state. For small Da the bars are not visible since the front speed is essentially constant in time after the transient acceleration period.

For small Da the front speed follows an approximately $\mathrm{Da}^{1/2}$ dependence. The stirring by the turbulent flow accelerates the propagation speed of the reaction-diffusion front by a constant factor, that is independent of Da:

$$S = v_T/v_0 \approx 9.5, \quad \mathrm{Da} \ll \tau_{\max}^{-1}. \tag{10}$$

Note also, that the acceleration factor S is independent of the details of the reaction dynamics defined by the source term $f(\theta)$. This shows that the acceleration factor in the slow reaction case is an inherent property of the transport processes. In this regime the chemical reaction is slower than the slowest eddies. The transport due to stirring, on time scales larger than the eddy turnover times of the largest (and slowest) eddies, can be described as a turbulent diffusion process. This suggests, that the front propagation speed can be obtained from the formula for the speed of the reaction-

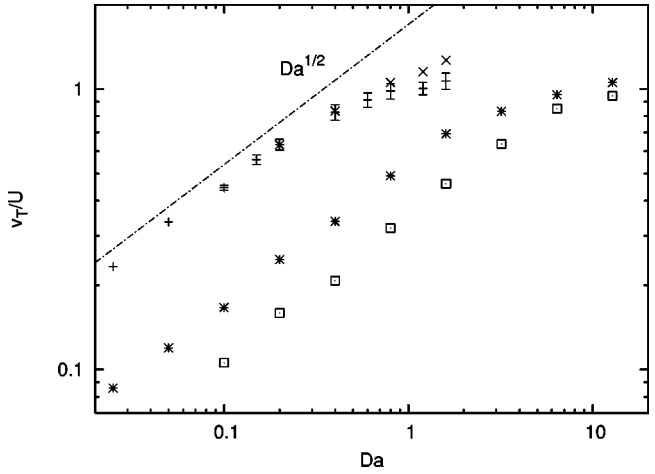

FIG. 6. Time averaged propagation speeds normalized by the root-mean-square (rms) turbulent velocity as of function of Da for three different types of reaction dynamics: $'+,\times'-\theta(1-\theta)$, $'*'-\theta^2(1-\theta)$, $'\boxdot'-(1-\theta)\exp(-1/\theta)$ and Pe=1244 except for the datapoints indicated by $\times$ that correspond to Pe=156. The vertical bars show the standard deviation of the fluctuations in time of the front speed for the quadratic autocatalytic reaction.

diffusion front in a stationary medium v_0 stated in the Introduction, by replacing the molecular diffusion coefficient with an effective turbulent diffusivity [22].

To test this prediction we measured the turbulent diffusivity numerically by observing the dispersion of a passive scalar (Da=0) along the channel due to the same turbulent flow. The initial distribution was chosen to be Gaussian along the channel and uniform in the transverse direction. Assuming that for long times and on length scales larger than the integral scale the dispersion is well modeled by a diffusive process the concentration averaged along the y axis ($\hat{\theta}$) should satisfy a diffusion equation

$$\frac{\partial \hat{\theta}}{\partial t} = D_T \Delta \hat{\theta} \tag{11}$$

with the solution

$$\hat{\theta}(x,t) = \frac{1}{\sqrt{t}} \exp \frac{-x^2}{4D_T t}, \tag{12}$$

where D_T is the turbulent diffusivity. By monitoring the increase of the width in time of the Gaussian profiles we obtained $D_T = 7.734 \times 10^{-2}$. Using this diffusivity in the laminar front speed formula we indeed obtain the measured values of the front speed for small Da with good approximation. Comparing D_T with the molecular diffusivity, in the same nondimensional units $D = \mathrm{Pe}^{-1} = 8.037 \times 10^{-4}$ we obtain a good estimate of the acceleration factor

$$S = \sqrt{D_T/D} \approx 9.8. \tag{13}$$

Still in the small Da regime, the propagation speed turns out to be relatively insensitive to moderate changes in the Peclét number. We decreased Pe up to a factor eight and did not observe any significant change in the front speed (Fig. 6).

This can be explained by the fact, that the effective turbulent diffusion is not affected by the molecular diffusion—it can be thought of as a noise term added to the fluid particle trajectories—as long as the molecular diffusion is much weaker than the diffusion due to the turbulent flow, i.e, Pe $\gg 1$.

For larger reaction rates, the reaction time scale Da^{-1} becomes comparable to the eddy turnover times related to the length scales defining the inverse energy cascade. The front propagation speed still increases with Da, but the increase is significantly slower than $\mathrm{Da}^{1/2}$. The enhancement of the front speed due to turbulence is indeed less efficient for fast reactions, $S=v_T/v_0<\sqrt{D_T/D}$. We propose the following explanation for this behavior. The reaction rate Da defines a characteristic length scale $l_0(\mathrm{Da})<L$ within the inertial range of the turbulent flow corresponding to eddies having a turnover time scale similar to the reaction time, $\tau_r \sim \mathrm{Da}^{-1}$. Eddies smaller than l_0 are faster than the chemical reaction and produce an effective turbulent diffusion. Eddies larger than l_0 on the other hand are too slow to be able to disperse the fluid parcels in the time needed for the reaction to complete and therefore, they lead to the wrinkling of the front structure as shown by the strong fluctuations of the scalar field in the transverse direction (Fig. 5). These eddies do not participate efficiently in the diffusive transport process, therefore the enhancement rate $S=v_T/v_0$ becomes smaller then the constant factor obtained for slow reactions and decreases with Da.

The front speed enhancement due to mixing (S) is shown in Fig. 7 as a function of the ratio between the rms turbulence velocity and the speed of the reaction-diffusion front $Q=U/v_0$. There have been various theoretical predictions for the $S(Q)$ relationship [32,33]. Our numerical results suggest a linear relationship $S=1+KQ$ ($K\approx 0.8$) in the regime of fast reactions (corresponding to small Q). In the large Q regime S is roughly constant as expected for the distributed reaction zone case discussed earlier. We also note, that in both regimes the data obtained from different types of reactions seem to collapse on the same curve.

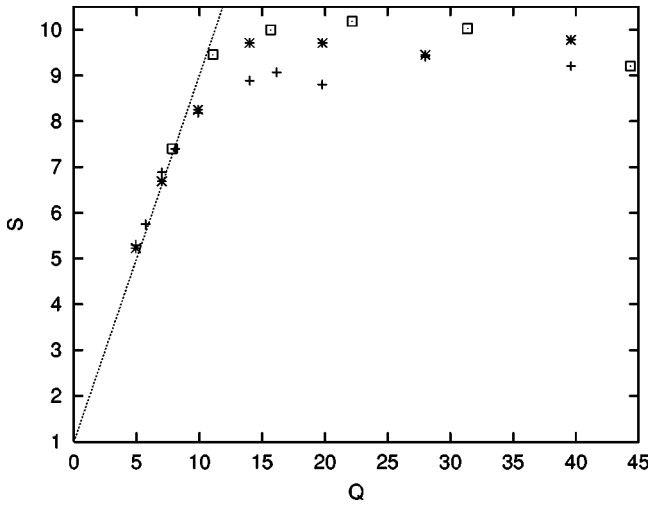

FIG. 7. Enhancement factor $S=v_T/U$ for all three types of reactions (using the same symbols as in Fig. 6) vs the ratio of the advection velocity and speed of the laminar propagation speed $Q=U/v_0$. The dashed line represents $S=1+08Q$.

IV. CONCLUSION

Using direct numerical simulations of two-dimensional turbulent flow we have found two characteristic regimes for front propagation. When the reaction is slower than all characteristic time scales of the turbulent velocity field, the front is broad with weak fluctuations in the transverse direction and the enhancement rate is independent of the Damköhler number Da. In the fast reaction regime, there is a relatively sharp wrinkled interface between the regions of fresh and fully consumed reactant. The turbulent mixing is less efficient in increasing the propagation speed as the reaction becomes faster. The transition between the two regimes takes place when the turbulent propagation speed becomes comparable to the characteristic velocity of the flow.

The slow reaction regime observed in our simulations is analogous to the one identified in Ref. [16] for the case of cellular laminar flows. For fast reactions it was found there that the propagation speed becomes independent of the Damköhler number. From our results it seems, that contrary to the case of cellular flows, in the turbulent flow the propagation speed continues to grow with Da, but more slowly than $\mathrm{Da}^{1/2}$. This difference appears to be a signature of the multiscale character of the flow. Establishing the exact form of the dependence of the propagation speed on Da in the fast reaction regime, requires numerical simulations with much higher resolution, able to resolve the very sharp front structure, and progress in theoretical understanding of the phenomenon.

[1] Z. Warhaft, Annu. Rev. Fluid Mech. **32**, 203 (2000).
[2] B. I. Shraimann and E. D. Siggia, Nature (London) **405**, 639 (2000).
[3] G. Falkovich, K. Gawedzki, and M. Vergassola, Rev. Mod. Phys. **73**, 913 (2001).
[4] See, for example, the special issue of Chaos 12, 2 (2002).
[5] I. Epstein and K. Showalter, J. Phys. Chem. **31**, 13132 (1996).
[6] Ya. B. Zeldovitch and D. A. Frank-Kamenetskii, Acta Physicochim. URSS **9**, 341 (1938).
[7] A. Linan and F. A. Williams, *Fundamental Aspects of Combustion* (Oxford University Press, Oxford, 1993).
[8] J. D. Murray, *Mathematical Biology* (Springer, Berlin, 1989).
[9] D. Vives, A. Careta, and F. Sagues, J. Chem. Phys. **107**, 7894 (1997).
[10] R. A. Fisher, Ann. Eugenics **7**, 355 (1937).
[11] A. Kolmogorov, I. Petrovsky, and N. Piskunov, Bull. Univ.

Moskou, Ser. Int. Sec. A **1**, 1 (1937).
[12] J. Xin, SIAM Rev. **42**, 161 (2000).
[13] U. Ebert and W. van Saarloos, Physica D **146**, 1 (2000).
[14] Z. Neufeld, P. H. Haynes, and T. Tél, Chaos **12**, 426 (2002).
[15] Z. Toroczkai, G. Károlyi, Á. Péntek, T. Tél, and C. Grebogi, Phys. Rev. Lett. **80**, 500 (1998).
[16] M. Abel, A. Celani, D. Vergni, and A. Vulpiani, Phys. Rev. E **64**, 046307 (2001).
[17] B. F. Edwards, Phys. Rev. Lett. **89**, 104501 (2002).
[18] M. Leconte, J. Martin, N. Rakotomalala, and D. Salin, Phys. Rev. Lett. **90**, 128302 (2003).
[19] P. Constantin, A. Kiselev, A. Oberman, and L. Rhyzik, Arch. Ration. Mech. Anal. **154**, 53 (2000).
[20] A. C. Marti, F. Sagues, and J. M. Sancho, Phys. Rev. E **56**, 1729 (1997).
[21] A. C. Marti, F. Sagues, and J. M. Sancho, Phys. Fluids **9**, 3851 (1997).
[22] G. Damköhler, Z. Elektrochem. Angew. Phys. Chem. **46**, 601 (1940).
[23] P. D. Ronney, B. D. Haslam, and N. O. Rhys, Phys. Rev. Lett. **74**, 3804 (1995).
[24] N. Peters, *Turbulent Combustion* (Cambridge University Press, Cambridge, 2000).
[25] M. Cencini, A. Torcini, D. Vergni, and A. Vulpiani, Phys. Fluids **15**, 679 (2003).
[26] M. Chertkov and V. Yakhot, Phys. Rev. Lett. **80**, 2837 (1998).
[27] R. H. Kraichnan, Phys. Fluids **10**, 1417 (1967).
[28] P. Tabeling, Phys. Rep. **362**, 1 (2002).
[29] S. Sukoriansky, B. Galperin, and A. Chekhlov, Phys. Fluids **11**, 3043 (1999).
[30] S. K. Lele, J. Comput. Phys. **103**, 16 (1992).
[31] T. Poinsot and D. Veynante, *Theoretical and Numerical Combustion* (R.T. Edwards, Philadelphia, 2001).
[32] V. Yakhot, Combust. Sci. Technol. **60**, 191 (1988).
[33] A. Pocheau, Phys. Rev. E **49**, 1109 (1994).